Supplementary Material for

ACQ ／AIE Transition of Rofecoxib-Based Analogues via Combined Ring Expansion and Amino Dimethylation Strategies and their Multiple Stimuli-Responsive Fluorescent Behaviors

Jingming Zhou, ‡[a] Yongbo Wei, ‡[a] Yu Cheng, ‡[b] Xia Wang, [a] Tong Wu, [a] Weiwei Zhang, [a] Yinyin Yao, [c] Yusheng Lu, *[c] Hongqiang Qiu *[b] and Lijun Xie *[a]

[a] *Fujian Provincial Key Laboratory of Screening for Novel Microbial Products, Fujian Institute of Microbiology, Fuzhou, Fujian 350007, P.R. China.*

[b] *Department of Pharmacy, Fujian Medical University Union Hospital, 29 Xin Quan Rd, Gulou, Fuzhou, 350001, Fujian, P.R. China.*

[c] *Fujian-Taiwan-Hongkong-Macao Science and Technology Cooperation Base of Intelligent Pharmaceutics, College of Material and Chemical Engineering, Minjiang University, Fuzhou, Fujian 350108, P.R. China.*

‡ These authors contributed equally to this work

* Corresponding author

Corresponding authors' e -mail: lu_yu_sheng@126.com (Y.L.),
hongqiangqiu@fjmu.edu.cn (H.Q.)
Lijunxie8224@outlook.com (L.X.)

Table of Contents

1. Experimental section 4
   1.1 Materials and Reagents 4
   1.2 Instruments 4
   1.3 Molecular design and synthesis 5
   1.4 Theoretical calculations 7
   1.5 X-Ray single-crystal diffraction 7
   1.6. Powder X-ray diffraction and thermal analysis 8
   1.7. Cell viability and live cell imaging on lipid droplets 8
      1.7.1 Cell Viability 8
      1.7.2 Cell Culture and Imaging in MCF-7 Cells 8
   1.8. Mechanochromism 9
      1.8.1 Grinding-immersing cycle 9
      1.8.2 Grinding-heating cycle 9
3. Supporting Figures and Tables. 10
   Figure S1. ^{1}H NMR of NF (600 MHz, DMSO-D_6). 10
   Figure S2. ^{13}C NMR of NF (151 MHz, DMSO-D_6). 10
   Figure S3. The HRMS spectra of NF. 11
   Figure S4. ^{1}H NMR of NHF (600 MHz, DMSO-D_6). 11
   Figure S5. ^{13}C NMR of NHF (151 MHz, DMSO-D_6). 12
   Figure S6. The HRMS spectra of NHF. 12
   Figure S7. ^{1}H NMR of F0 (600 MHz, DMSO-D_6). 13
   Figure S8. ^{13}C NMR of F0 (151 MHz, DMSO-D_6). 13
   Figure S9. The HRMS spectra of F0. 14
   Figure S10. ^{1}H NMR of FA (600 MHz, DMSO-D_6). 14
   Figure S11. ^{13}C NMR of FA (151 MHz, DMSO-D_6). 15
   Figure S12. The HRMS spectra of FA. 15
   Figure S13. ^{1}H NMR of FB (600 MHz, DMSO-D_6). 16
   Figure S14. ^{13}C NMR of FB (151 MHz, DMSO-D_6). 16
   Figure S15. The HRMS spectra of FB. 17
   Figure S16. ^{1}H NMR of FAB (600 MHz, chloroform-*D*). 17
   Figure S17. ^{13}C NMR of FAB (151 MHz, chloroform-*D*). 18
   Figure S18. The HRMS spectra of FAB. 18
   Figure S19. Absorption spectra of compounds F0(A), FA(B), FB(C) and FAB(D) in different solvents. (c = 50 μM) 19
   Figure S20. Absorption spectra of compounds F0(A), FA(B), FB(C) and FAB(D) in water−DMSO mixtures with different water fractions (c = 10 μM). 19
   Table S1. Crystal data and structure refinement for FA, FB and FAB. 20
   Table S2. Fractional Atomic Coordinates (×10^4) and Equivalent Isotropic Displacement Parameters (Å^2×10^3) for FA. U_{eq} is defined as 1/3 of the trace of the orthogonalised U_{IJ} tensor. 21
   Table S3. Fractional Atomic Coordinates (×10^4) and Equivalent Isotropic Displacement Parameters (Å^2×10^3) for FB. U_{eq} is defined as 1/3 of the trace of the orthogonalised U_{IJ} tensor. 22
   Table S4. Fractional Atomic Coordinates (×10^4) and Equivalent Isotropic Displacement Parameters (Å^2×10^3) for FAB. U_{eq} is defined as 1/3 of the trace of the orthogonalised U_{IJ} tensor. 23
   Figure S21. Stacking structure (A, B) and diagram(C) of FA. 24
   Figure S22. Stacking structure (A, B, C) and diagram(D) of FB. 24

Figure S23. Stacking structure (A, C) and diagram (B, D) of FAB. 25
Figure S24. Cell viability values (%) estimated by CCK8 assays using MCF-7 and Hela cells, cultured in the presence of 0.01-50 μM of FAB for 24 h at 37 °C 26

1. Experimental section

1.1 Materials and Reagents

2'-Bromoacetophenone was purchased from Shanghai Energy Chemical Co., Ltd, China. 4-Nitrophenylacetic acid and 2-(1H-Pyrrol-1-yl)benzaldehyde was purchased from Shanghai Bide Pharmaceutical Technology Co., Ltd, China. 2-(Piperidin-1-yl)benzaldehyde was purchased from Hubei Yunmei Technology Co., Ltd, China. 1,8-diazabicyclo[5.4.0]undec-7-ene (DBU) was purchased from Shanghai Aladdin Biochemical Technology Co., Ltd, China. Zinc powder was purchased from Sigma Aldrich (Shanghai) Trading Co., Ltd, China. Chemical solvents such as acetonitrile, triethylamine, trifluoroacetic acid (TFA), hydrochloric acid, acetone, dichloromethane (DCM), ethanol (EtOH), tetrahydrofuran (THF), N,N-dimethylformamide (DMF), methanol (MeOH), dimethyl sulfoxide (DMSO), chloroform, petroleum ether (60−90 ℃), piperidine, ethyl acetate , formaldehyde, formic acid, ammonium chloride, sodium bicarbonate ,anhydrous sodium sulfate and sodium chloride were purchased from Sinopharm Chemical Reagent Co. Ltd, China. All chemicals were used as received without further purification unless otherwise claimed.

1.2 Instruments

Fluorescence spectra were recorded on a Varioskan LUX 3020–80110. Differential scanning calorimetry (DSC) traces were obtained on a DSC STAR system at a heating rate of 10 ℃/min from 40 ℃ to 300 ℃ under a high purity nitrogen atmosphere. Powder X-ray diffraction (PXRD) patterns were recorded on a Rigaku (D/MaX-3B) diffractometer. Crystal Structure Determination: SXRD was conducted with Bruker D8 Quesr/Venture diffraction with λ = 0.71 Å (MoKα). ^{1}H NMR and ^{13}C NMR spectra were measured on a Bruker AV 600 spectrometer in appropriated deuterated DMSO or DCM solution at room temperature with the solvent residual proton signal as a standard. High-resolution mass spectra (HRMS) were obtained on an Agilent 6545 Q-TOF LCMS. The datas of cell viability were collected on a multifunctional microplate reader (TECAN, M200 PRO, Switzerland). A Lipid droplets (LDs) imaging was performed with a confocal microscope (Leica, STELLARIS 5, Germany).

1.3 Molecular design and synthesis

In this study, we have designed and synthesized a new class of several AIE-active molecules with two subtle structural modification on the structure of ACQ molecule **F0**. The non-π-conjugated region of **F0** consists mainly of an amino group and a pyrrole ring. **FA**, **FB** and **FAB** compounds were designed by using piperidine ring instead of pyrrole ring for ring expansion and dimethylamino group instead of amino group (as show in TOC). The synthesis route is shown in Scheme 1, and the specific operations are as follows:

Synthesis of NF. 2'-Bromoacetophenone (2.0067 g, 0.010 mol) and 4-Nitrophenylacetic acid (1.8115 g, 0.010 mol) were dissolved in acetonitrile (30 mL), and then, triethylamine (3.0357g, 0.030 mol) was added. The reaction was stirred for about 0.5 h at room temperature. Next, the solution was transferred to salt ice bath at −5 ℃. Then, DBU (2.2836 g, 0.015 mol) was poured into the mixture and stirred for another 15 min at room temperature until the reaction was done. The reaction process was monitored in real time with TLC, dilute hydrochloric acid (1mol/L) was added after the reaction is complete, dichloromethane was extracted 3 times, the organic phase was combined, the organic layer was washed with saturated sodium bicarbonate solution, and then washed with saturated saline 1 time, the dichloromethane layer was collected, dried with anhydrous sodium sulfate for 1 hour, filtered to remove anhydrous sodium sulfate, and distilled under reduced pressure to obtain crude products. After that, the solid powder was recrystallized in ethanol to get the key intermediate **NF** as yellow powder. Yield: 52%.

Compound **NF.** ^{1}H NMR (600 MHz, DMSO-D_6) δ 8.31 – 8.25 (m, 2H), 7.66 – 7.60 (m, 2H), 7.51 – 7.45 (m, 1H), 7.42 (ddt, J = 7.3, 6.3, 1.4 Hz, 2H), 7.40 – 7.36 (m, 2H), 5.46 (s, 2H).^{13}C NMR (151 MHz, DMSO-D_6) δ 172.3, 160.3, 147.3, 137.5, 131.0, 130.9, 130.6, 130.1, 129.1, 128.9, 127.8, 123.8, 123.0, 71.2. HRMS- ESI (*m/z*): $[M+H]^+$ calcd for $C_{16}H_{11}NO_4$, 282.0722; found, 282.0775.

Synthesis of NHF. Add starting material **NF** (500.0 mg, 1.78 mmol) and zinc powder (578.0 mg, 8.9 mmol) to absolute ethanol (10.0 mL) and stir for 30 min at 65 ℃. Then, ammonium chloride (472 mg, 8.9 mmol) and water (10 mL) is added to the mixture with further agitation for 4 h at 65 ℃. Filter out the insoluble matter and wash and concentrate the filtrate with dichloromethane, add excess saturated sodium bicarbonate to the residue, dichloromethane extraction three times, dry the extract with anhydrous sodium sulfate, concentrate the extract, and distill to obtain the compound **NHF** (68% yield). The precipitation was observed and then filtered to get the targets, which were dried under vacuum at 60 ℃ for 4 h.

Compound **NHF.** ^{1}H NMR (600 MHz, DMSO-D_6) δ 7.48 – 7.34 (m, 5H), 7.07 – 6.98 (m, 2H), 6.59 – 6.51 (m, 2H), 5.26 (s, 2H), 3.35 (s, 2H). ^{13}C NMR (151 MHz, DMSO-D_6) δ 173.6, 154.0, 149.1, 131.5, 130.1, 129.9, 128.8,

127.5, 124.9, 116.9, 113.6, 70.4. HRMS- ESI (*m/z*): $[M+H]^+$ calcd for $C_{16}H_{13}NO_2$, 252.0980; found, 252.1030.

Synthesis of F0. The obtained brown solid powder **NHF** (200.0 mg, 0.80 mmol) and two-fold equivalent of 2-(1H-Pyrrol-1-yl)benzaldehyde (274.0 mg, 1.6 mmol) were dissolved in methanol (10 mL). Then, piperidine as a catalyst was added (two drops). The reaction was stirred for 12 h at room temperature. The precipitation was formed and then filtered to get the crude products. By TLC (petroleum ether: ethyl acetate = 2:1) purification, the product **F0** is obtained (51% yield).

Compound **F0.** ^{1}H NMR (600 MHz, DMSO-D_6) δ 7.86 (dd, *J* = 7.8, 1.6 Hz, 1H), 7.59 – 7.47 (m, 3H), 7.46 – 7.35 (m, 2H), 7.30 – 7.16 (m, 1H), 7.17 – 7.09 (m, 2H), 7.02 – 6.89 (m, 2H), 6.48 – 6.40 (m, 2H), 5.97 (s, 1H), 5.48 (d, *J* = 10.2 Hz, 2H), 3.06 – 2.98 (m, 4H), 1.79 – 1.68 (m, 4H). ^{13}C NMR (151 MHz, DMSO-D_6) δ 169.1, 150.1, 150.1, 150.0, 147.6, 146.4, 131.8, 131.4, 130.3, 130.0, 129.7, 129.5, 129.4, 124.1, 124.0, 120.9, 117.0, 116.6, 113.8, 113.7, 109.6, 52.5, 40.1, 24.8. HRMS- ESI (*m/z*): $[M+H]^+$ calcd for $C_{27}H_{24}N_2O_2$, 409.1871; found, 409.1924.

Synthesis of FA. In a round-bottom flask, the obtained brown solid powder **NHF** (200.2 mg, 0.80 mmol) and two-fold equivalent of 2-(Piperidin-1-yl)benzaldehyde (302.8 mg, 1.6 mmol) were mixed in methanol (10 mL). Then, piperidine as a catalyst was added and stirred the mixture at ambient temperature for 12 h. The precipitation was formed and then filtered using suction pump, washed with ethanol, and dried to get the crude products. By TLC (petroleum ether: ethyl acetate = 2:1) purification, the product **FA** is obtained (43% yield).

Compound **FA.** ^{1}H NMR (600 MHz, DMSO-D_6) δ 8.01 (d, *J* = 7.8 Hz, 1H), 7.58 – 7.52 (m, 3H), 7.43 – 7.39 (m, 2H), 7.28 (t, *J* = 7.7 Hz, 1H), 7.13 (t, *J* = 8.3 Hz, 3H), 7.04 (d, *J* = 8.1 Hz, 1H), 6.44 (d, *J* = 8.3 Hz, 2H), 6.18 (s, 1H), 5.50 (d, *J* = 10.2 Hz, 2H), 2.74 (d, *J* = 6.6 Hz, 4H), 1.38 (d, *J* = 14.5 Hz, 6H), .^{13}C NMR (151 MHz, DMSO-D_6) δ 168.5, 153.0, 149.6, 148.1, 146.0, 131.3, 130.4, 129.8, 129.6, 129.2, 129.1, 129.0, 126.7, 123.8, 122.7, 119.1, 116.0, 113.2, 113.2, 107.1, 53.7, 25.8, 23.6. HRMS- ESI (*m/z*): $[M+H]^+$ calcd for $C_{28}H_{26}N_2O_2$, 423.2028; found, 423.2068.

Synthesis of FB. In a round-bottom flask, the solid powder **F0** (100.0 mg, 0.25 mmol), four-fold equivalent of formaldehyde (30.0 mg, 1.0 mmol) and six-fold equivalent of formic acid (69.0 mg, 1.5 mmol) were mixed in tetrahydrofuran (10 mL). The mixture were stirred at 60 ℃ for 12 h. The reaction process was monitored in real time with TLC. After the end of the reaction, saturated sodium bicarbonate is added to neutralize formic acid, extracted with dichloromethane, and the reaction solution is concentrated to obtain a crude product. The crude mixture was filtered through celite and chromatographed using silica (200-300 mesh), eluted using petroleum ether /ethyl acetate (2:1 v/v) is used to obtain a pure product **FB**. (65% yield)

Compound **FB.** ^{1}H NMR (600 MHz, DMSO-d6) δ 7.87 (d, J = 7.8 Hz, 1H), 7.54 (d, J = 6.5 Hz, 3H), 7.42 (d, J = 6.7 Hz, 2H), 7.29 (d, J = 8.4 Hz, 2H), 7.22 (t, J = 7.8 Hz, 1H), 7.00 – 6.92 (m, 2H), 6.61 (d, J = 8.5 Hz, 2H), 5.97 (s, 1H), 3.03 (s, 4H), 2.90 (s, 6H), 1.74 (s, 4H), . ^{13}C NMR (151 MHz, DMSO) δ 169.1, 150.7, 150.0, 147.5, 146.7, 131.7, 131.3, 130.0, 130.0, 129.8, 129.5, 129.4, 124.0, 123.6, 120.8, 116.9, 116.8, 112.0, 109.8, 52.4, 24.7. HRMS- ESI (*m/z*): $[M+H]^+$ calcd for $C_{29}H_{28}N_2O_2$, 437.2184; found, 437.2223.

Synthesis of FAB. In a round-bottom flask, the solid powder **FA**(100 mg, 0.24 mmol), four-fold equivalent of formaldehyde (28.8 mg, 0.96 mmol) and six-fold equivalent of formic acid (66.2 mg, 1.44 mmol) were mixed in tetrahydrofuran (10 mL). The mixture were stirred at 60 ℃ for 12 h. The reaction process was monitored in real time with TLC. After the end of the reaction, saturated sodium bicarbonate is added to neutralize formic acid, extracted with dichloromethane, and the reaction solution is concentrated to obtain a crude product. The crude mixture was filtered through celite and chromatographed using silica (200-300 mesh), eluted using petroleum ether /ethyl acetate (2:1 v/v) is used to obtain a pure product **FAB**. (60% yield).

Compound **FAB.** ^{1}H NMR (600 MHz, CHLOROFORM-*D*) δ 8.24 (dd, *J* = 7.8, 1.6 Hz, 1H), 7.53 – 7.36 (m, 7H), 7.29 – 7.19 (m, 1H), 7.13 – 7.04 (m, 1H), 6.97 (dd, *J* = 8.0, 1.2 Hz, 1H), 6.63 – 6.54 (m, 2H), 6.38 (s, 1H), 2.95 (d, *J* = 0.8 Hz, 6H), 2.81 (d, *J* = 8.1 Hz, 4H), 1.45 (s, 6H). ^{13}C NMR (151 MHz, CHLOROFORM-*D*) δ 169.7, 153.6, 150.4, 148.6, 146.9, 132.1, 131.6, 130.2, 129.5, 129.1, 129.0, 127.7, 124.2, 123.0, 118.8, 117.4, 111.7, 108.6, 54.3, 40.2, 26.4, 24.3. HRMS- ESI (*m/z*): $[M+H]^+$calcd for $C_{30}H_{30}N_2O_2$, 451.2341; found, 451.2382.

The structure of **NF**, **NHF**, **F0**, **FA**, **FB** and **FAB** were characterized and confirmed by ^{1}H NMR, ^{13}C NMR, and HRMS (Figure. S1–S18).

1.4 Theoretical calculations

Using the Gaussian 09 program at the B3LYP and density functional theory (DFT) calculated the orbital energy of the optimized **F0, FA, FB** and **FAB** to understand the spectral behaviour. The single-molecular ground-state geometry was optimize using the B3LYP functional and the 6–311++G (2d, p) basis set to obtain geometry of the optimize **F0, FA, FB** and **FAB**.

1.5 X-Ray single-crystal diffraction

Obtaining crystal samples of the **FA**, **FB** and **FAB** through recrystallizing their powder in acetone, acetone and ethyl acetate, respectively. Crystal Structure Determination: SXRD was conducted with CrysAlisPro 1.171.40.39a (Rigaku OD, 2019) with λ = 0.71 Å (MoKα) for **FA** and **FB**, λ = 1.34 Å (MoKα) for **FAB**. The structures were solved by direct methods using SHELXS-97

and refined by full matrix least-squares with SHELXL-97. Using the olex2 software to calculated the intermolecular stacking distance of the crystal. X-ray Crystallography CCDC No. 2284607, CCDC No. 2284616 and CCDC No. 2284543 contains the supplementary crystallographic data for this paper.

1.6. Powder X-ray diffraction and thermal analysis

Powder X-ray diffraction (PXRD) patterns were recorded on the X'Pert3 Powder. Differential scanning calorimetry (DSC) traces were obtained on a DSC STAR system at a heating rate of 10 °C/min from 40 °C to 300 °C under a high purity nitrogen atmosphere.

1.7. Cell viability and live cell imaging on lipid droplets

1.7.1 Cell Viability

All the culture medium used in cell culture was purchased from ThermoFisher Scientific. MCF-7 and Hela cells were cultured at a density of 5×10^3 cells per well in a 96-well plate for 72 hours. Then the cells were treated with the medium containing diverse concentration of **FAB** for 24 hours, 10 μL of Cell Counting Kit - 8 (CCK8, DOJINDO, Japan) was added to the cells, and the incubation was continued for 1 hour at 37°C. The cell viability was determined by measuring the absorbance at 490 nm using a multifunctional microplate reader (TECAN, M200 PRO, Switzerland), and the results were expressed as the relative ratio of cell viability in comparison with the untreated control.

1.7.2 Cell Culture and Imaging in MCF-7 Cells

MCF-7 cells were cultivated on a confocal dish for 24 hours. Then, the culture medium was substituted with a medium that contained 10 μM **FAB** as well as BODIPY503. After incubation for 30 min, these cells were washed with PBS and resuspended in fresh medium. Then images were immediately acquired using a confocal microscope (Leica, STELLARIS 5, Germany), employing consistent acquisition parameters across all experimental groups. Green Channel of BODIPY503 was at 500-550 nm with excitation at 488 nm. Red Channel of **FAB** were at 575-840 nm with excitation at 488 nm. The Data on co-localization parameters were all calculated by the ImageJ software package.

1.8. Mechanochromism

1.8.1 Grinding-immersing cycle

1. The original **FAB** powder was placed in an agate mortar and photographed under a hand-held UV lamp light at 365 nm (8 W, 306 μW/cm^2). A small amount of raw powder was scanned to obtain the original solid fluorescence emission spectrum.

2. The **FAB** powder was ground with a pestle until it was completely discolored. The powder was then photographed under the hand-held UV lamp (365 nm, 8 W, 306 μW/cm²), and a small amount was taken for solid-state fluorescence emission spectrum scanning.

3. A small amount of acetone was added to the mortar to soak the ground **FAB** powder, allowing the color of the powder to return to its original state. After the acetone had evaporated, the powder was photographed again under the hand-held UV lamp (365 nm, 8 W, 306 μW/cm²), and a small amount was taken for solid-state fluorescence emission spectrum scanning.

4. Steps 2 and 3 were repeated, and a reversible color change cycle was observed.

1.8.2 Grinding-heating cycle

1. The original **FAB** powder was placed in an agate mortar and photographed under a hand-held UV lamp light at 365 nm (8 W, 306 μW/cm^2). A small amount of raw powder was scanned to obtain the original solid fluorescence emission spectrum.

2. The **FAB** powder was ground with a pestle until it was completely discolored. The powder was then photographed under the hand-held UV lamp (365 nm, 8 W, 306 μW/cm²), and a small amount was taken for solid-state fluorescence emission spectrum scanning.

3. Place the mortar in the oven and heat it at 90°C for 20 minutes. After removing it from the oven, allow it to cool in a desiccator. The color of the **FAB** powder will be observed to return to its original state. Photograph the powder under a hand-held UV lamp (365 nm, 8 W, 306 μW/cm²), and then scan a small amount of the powder to obtain the solid fluorescence emission spectrum.

4. Steps 2 and 3 were repeated, and a reversible color change cycle was observed.

3. Supporting Figures and Tables.

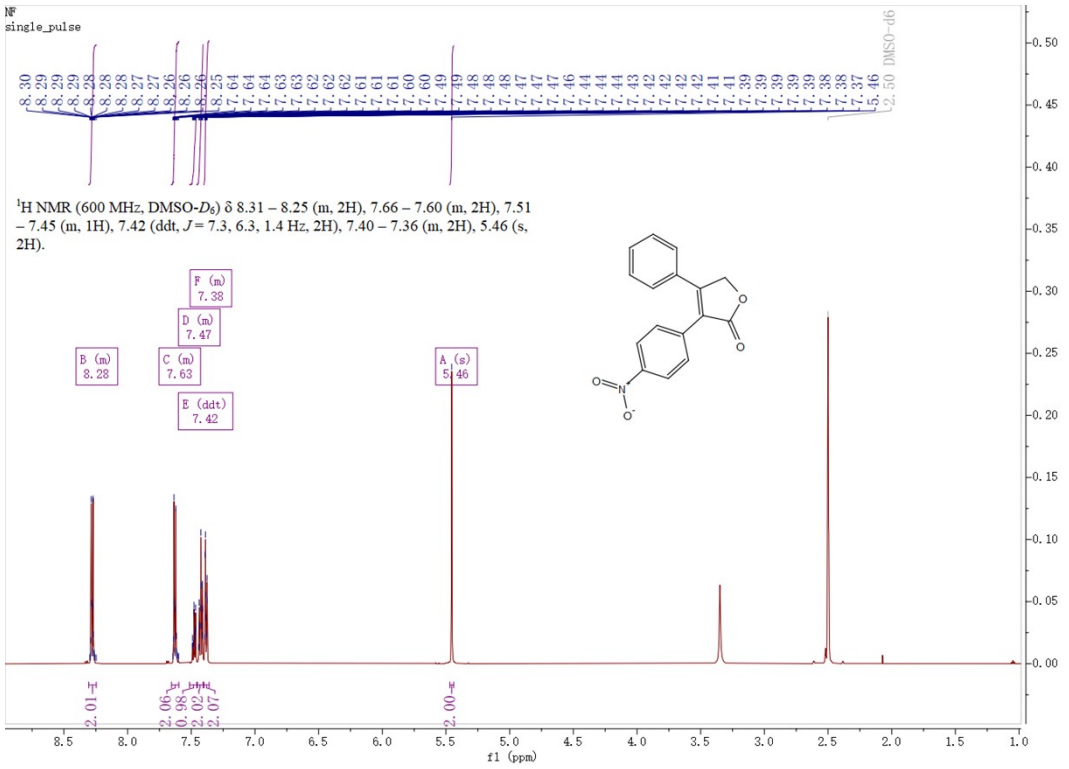

Figure S1. ^{1}H NMR of NF (600 MHz, DMSO-D_6).

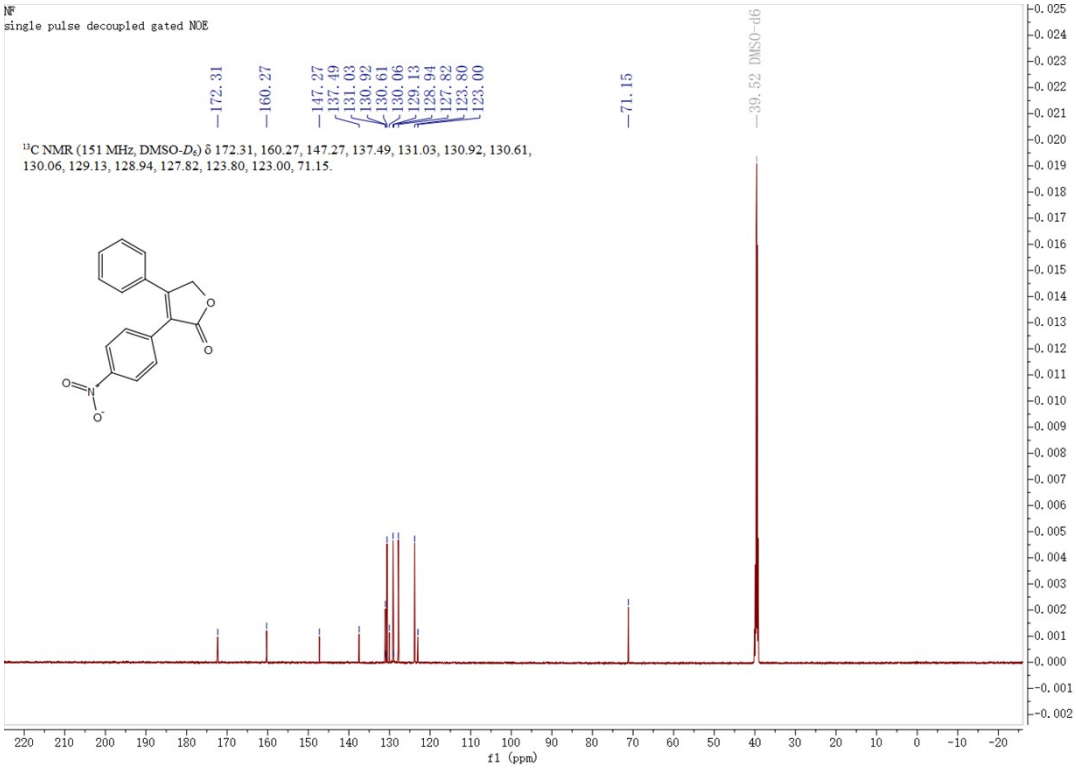

Figure S2. ^{13}C NMR of NF (151 MHz, DMSO-D_6).

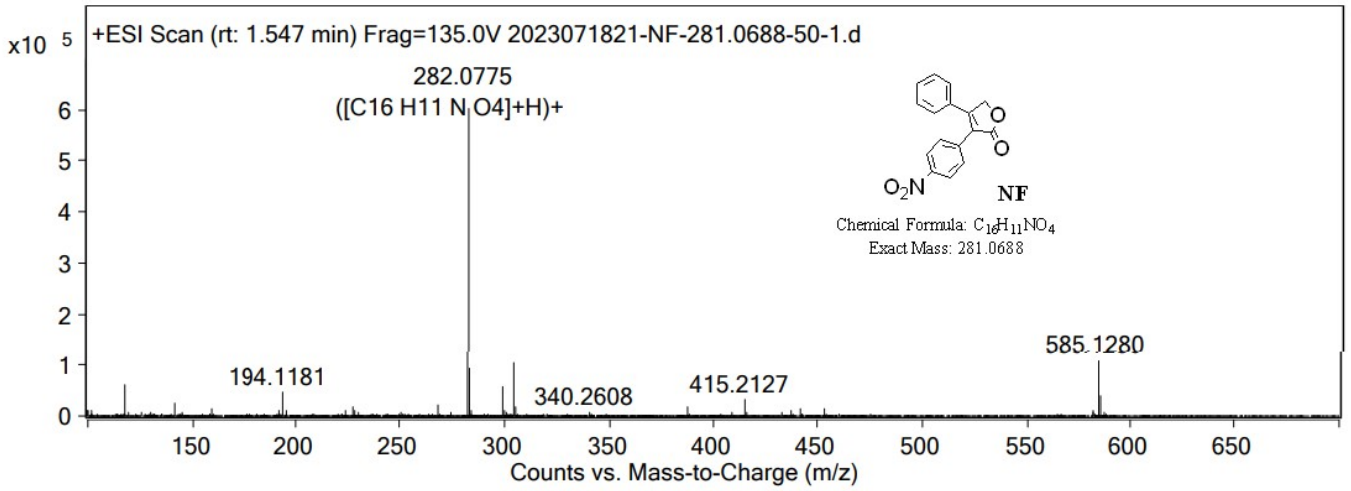

Figure S3. The HRMS spectra of NF.

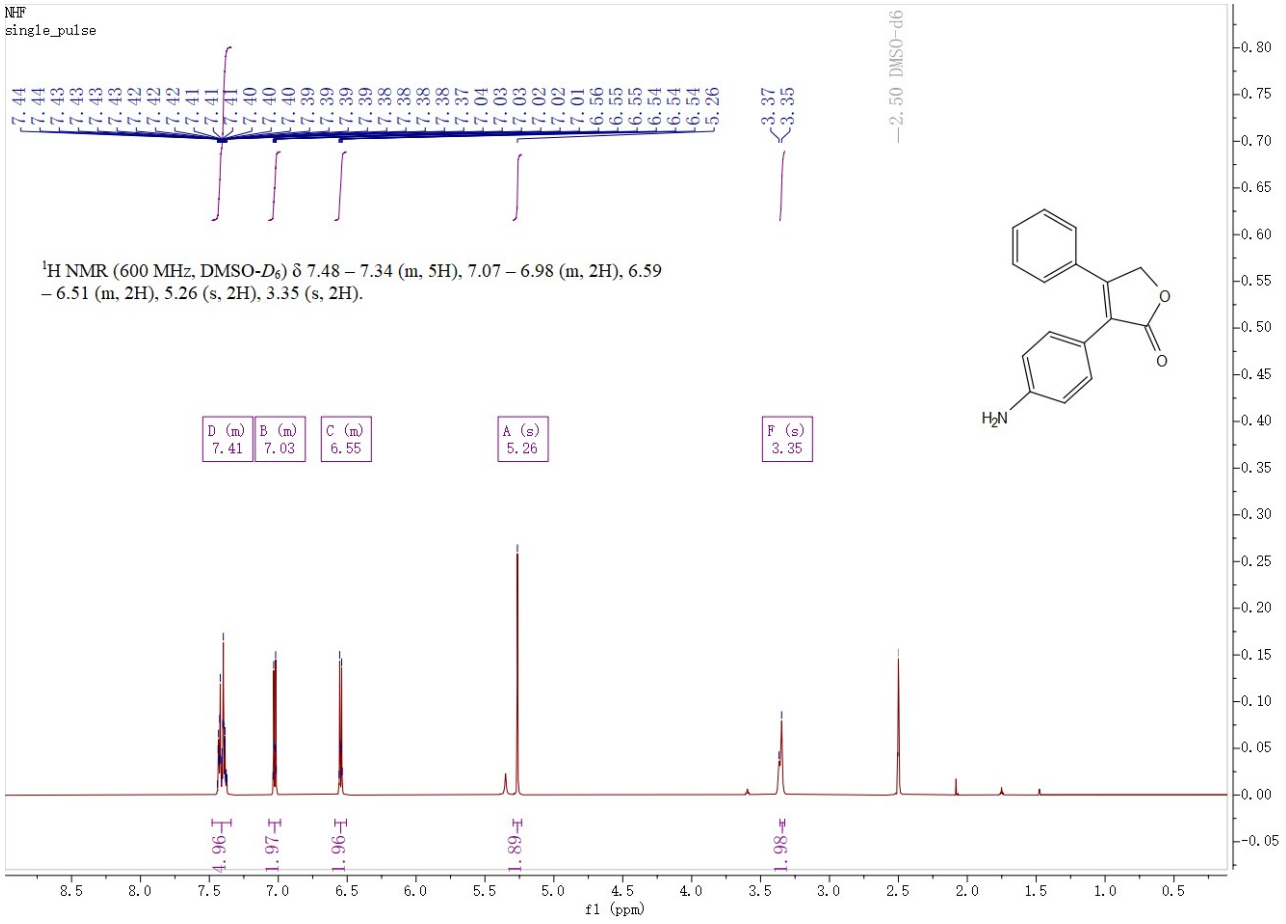

Figure S4. ^{1}H NMR of NHF (600 MHz, DMSO-D_6).

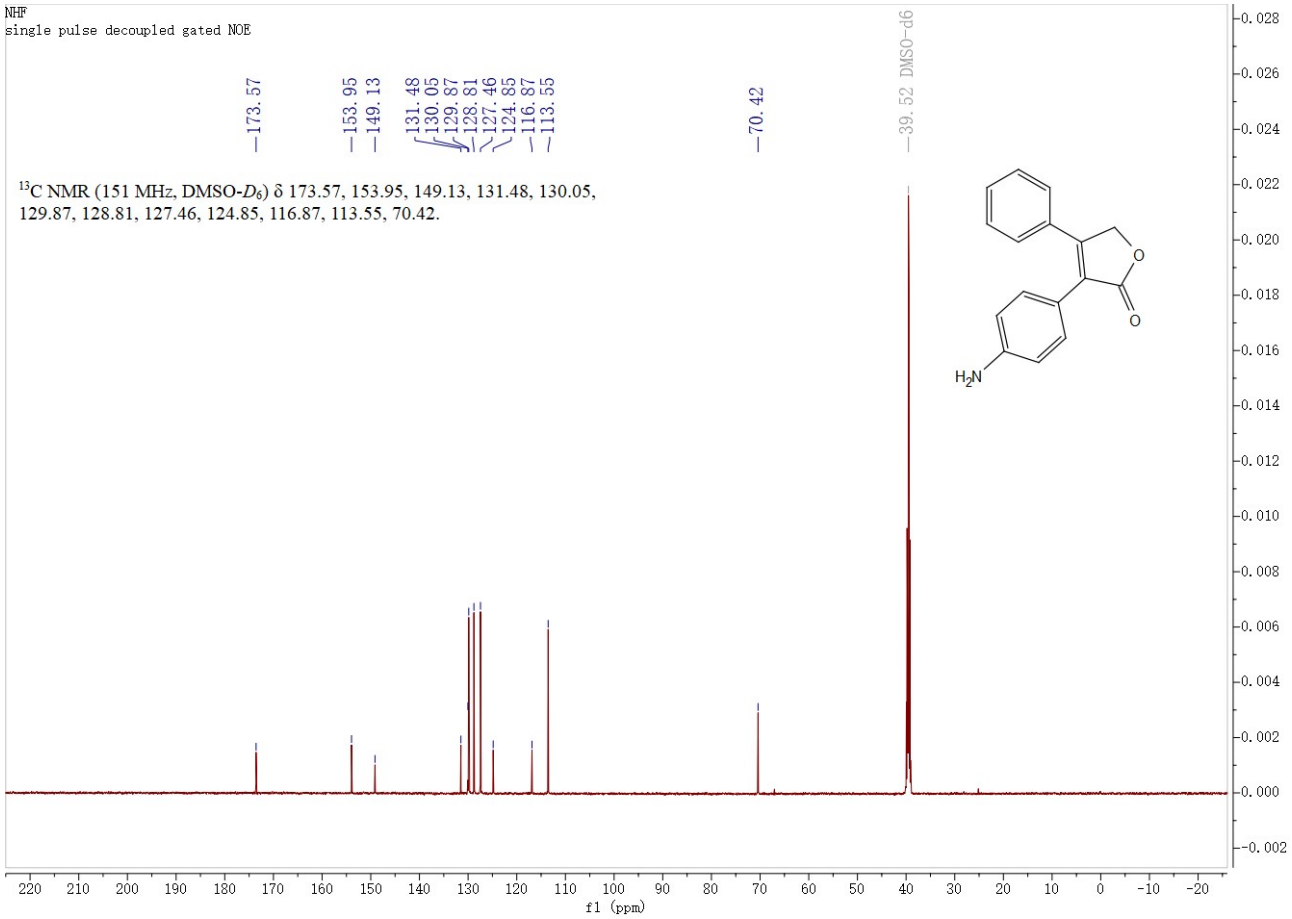

Figure S5. ^{13}C NMR of NHF (151 MHz, DMSO-D_6).

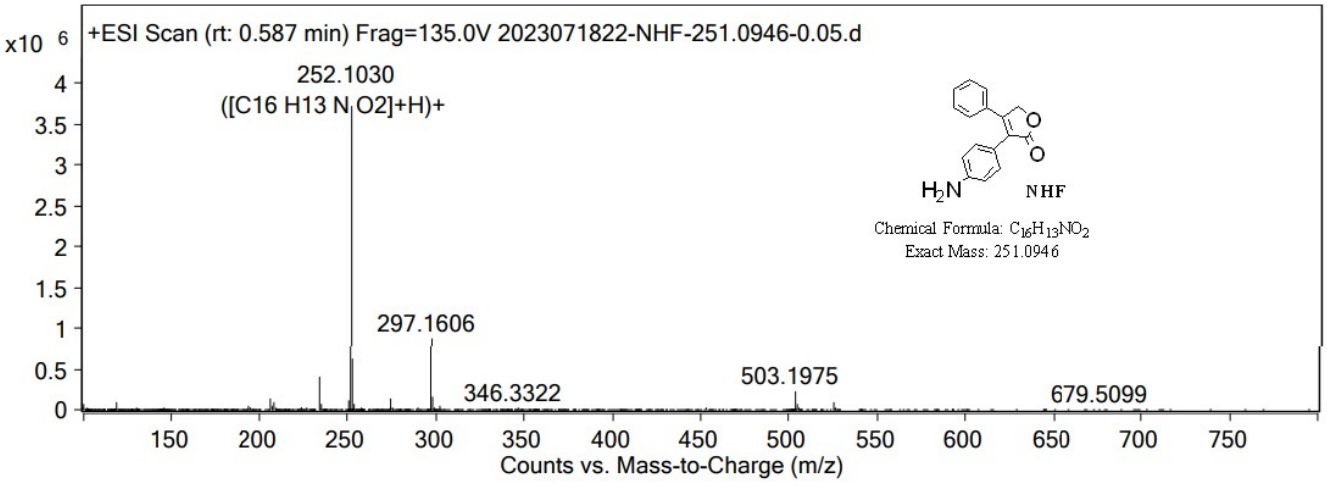

Figure S6. The HRMS spectra of NHF.

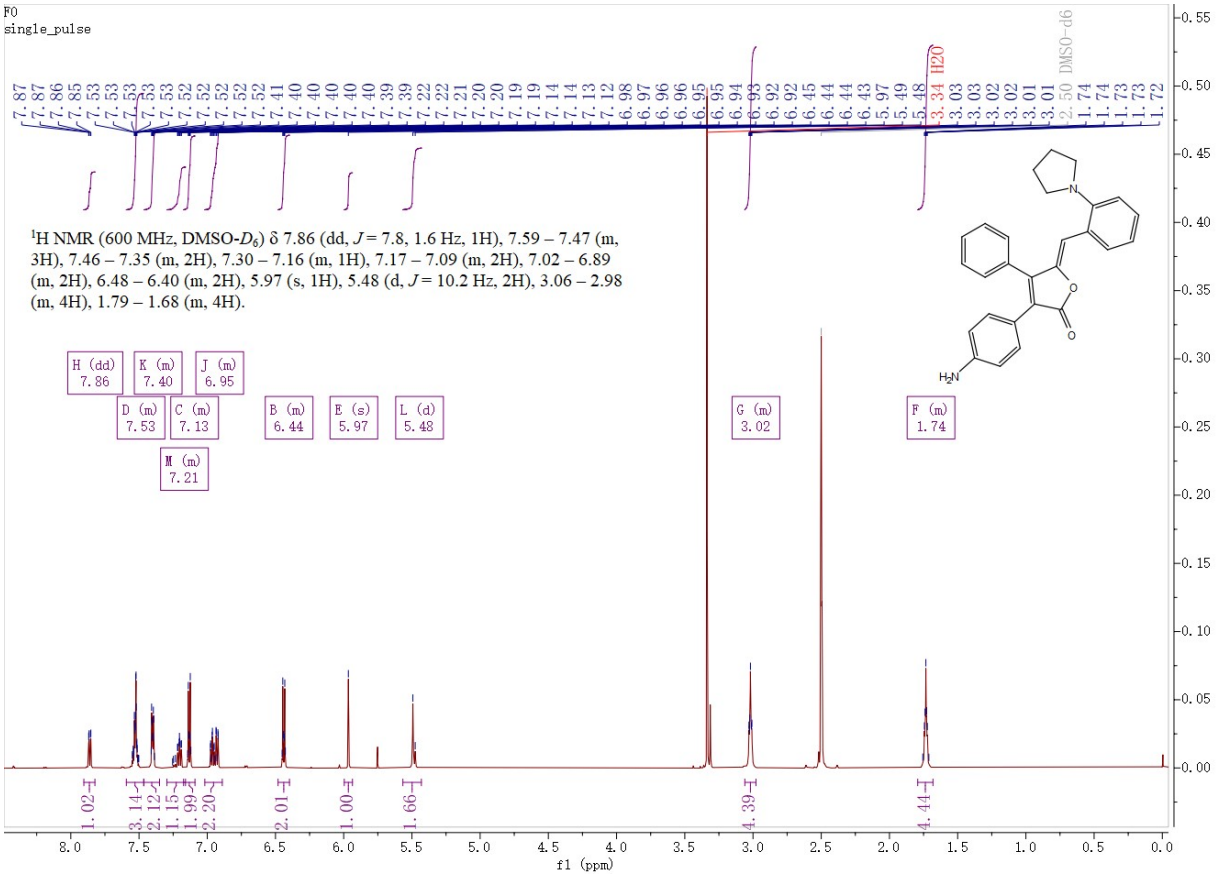

Figure S7. ^{1}H NMR of F0 (600 MHz, DMSO-D_6).

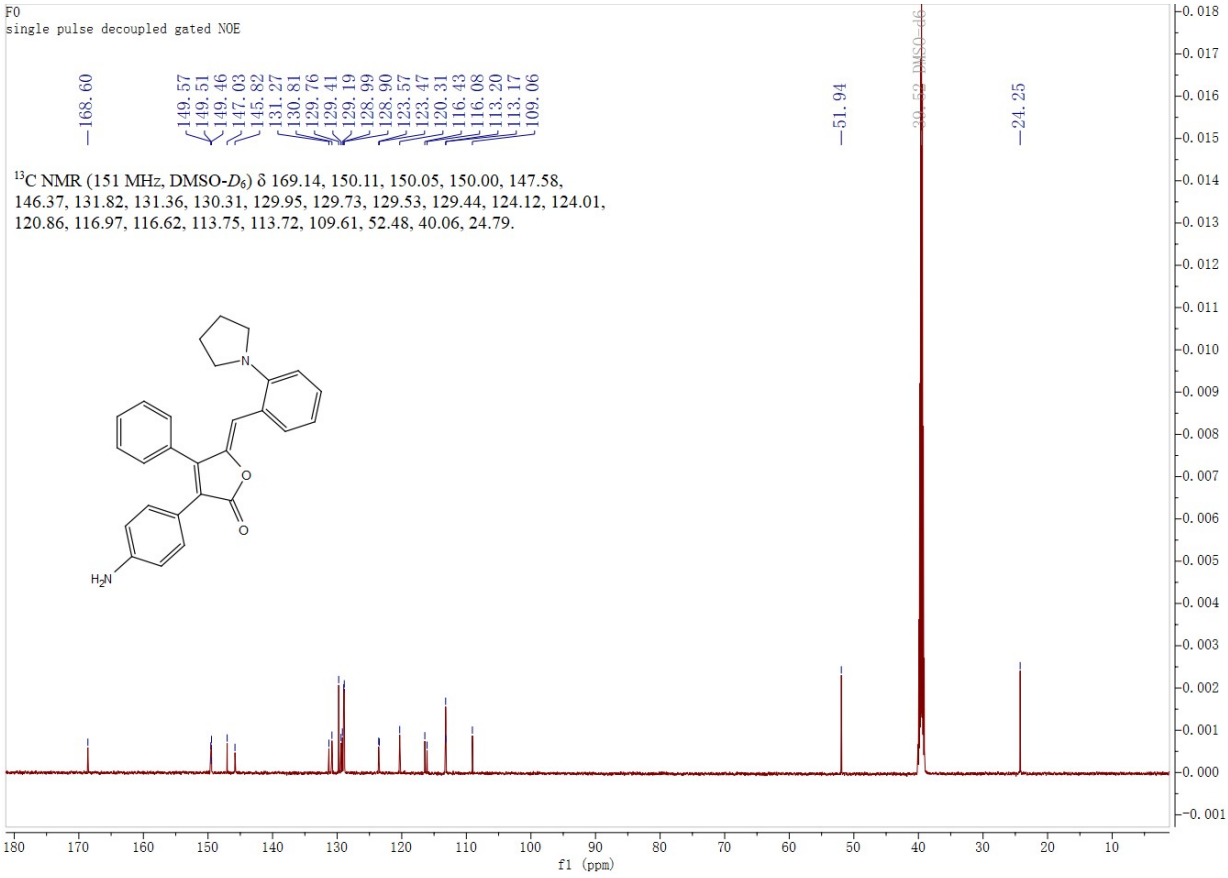

Figure S8. ^{13}C NMR of F0 (151 MHz, DMSO-D_6).

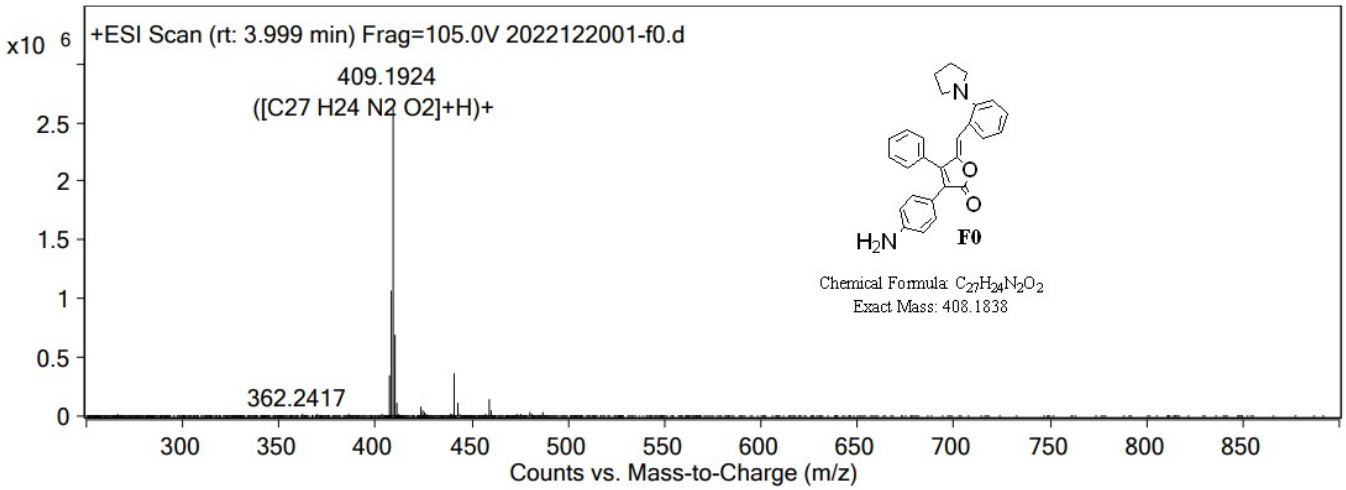

Figure S9. The HRMS spectra of F0.

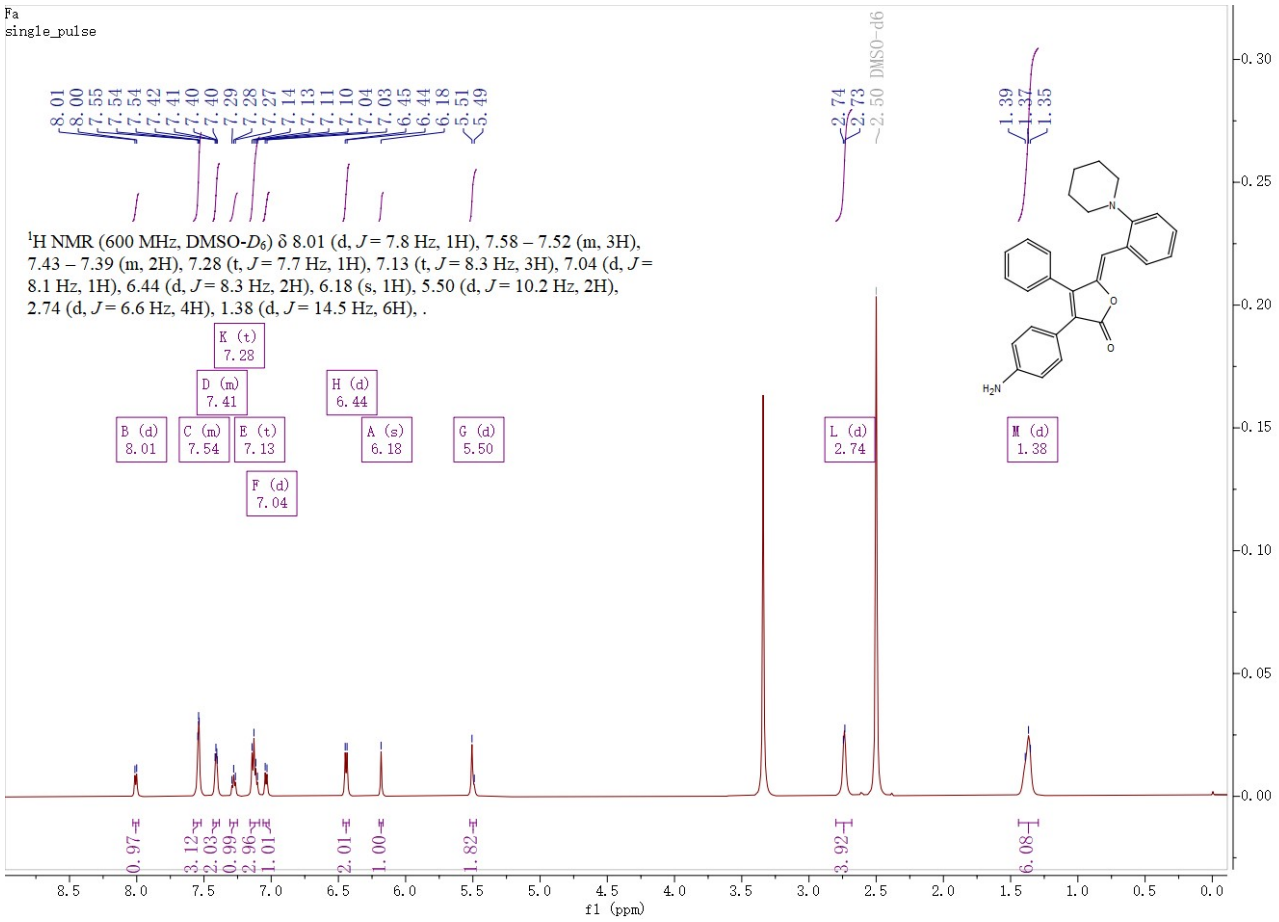

Figure S10. ^{1}H NMR of FA (600 MHz, DMSO-D_6).

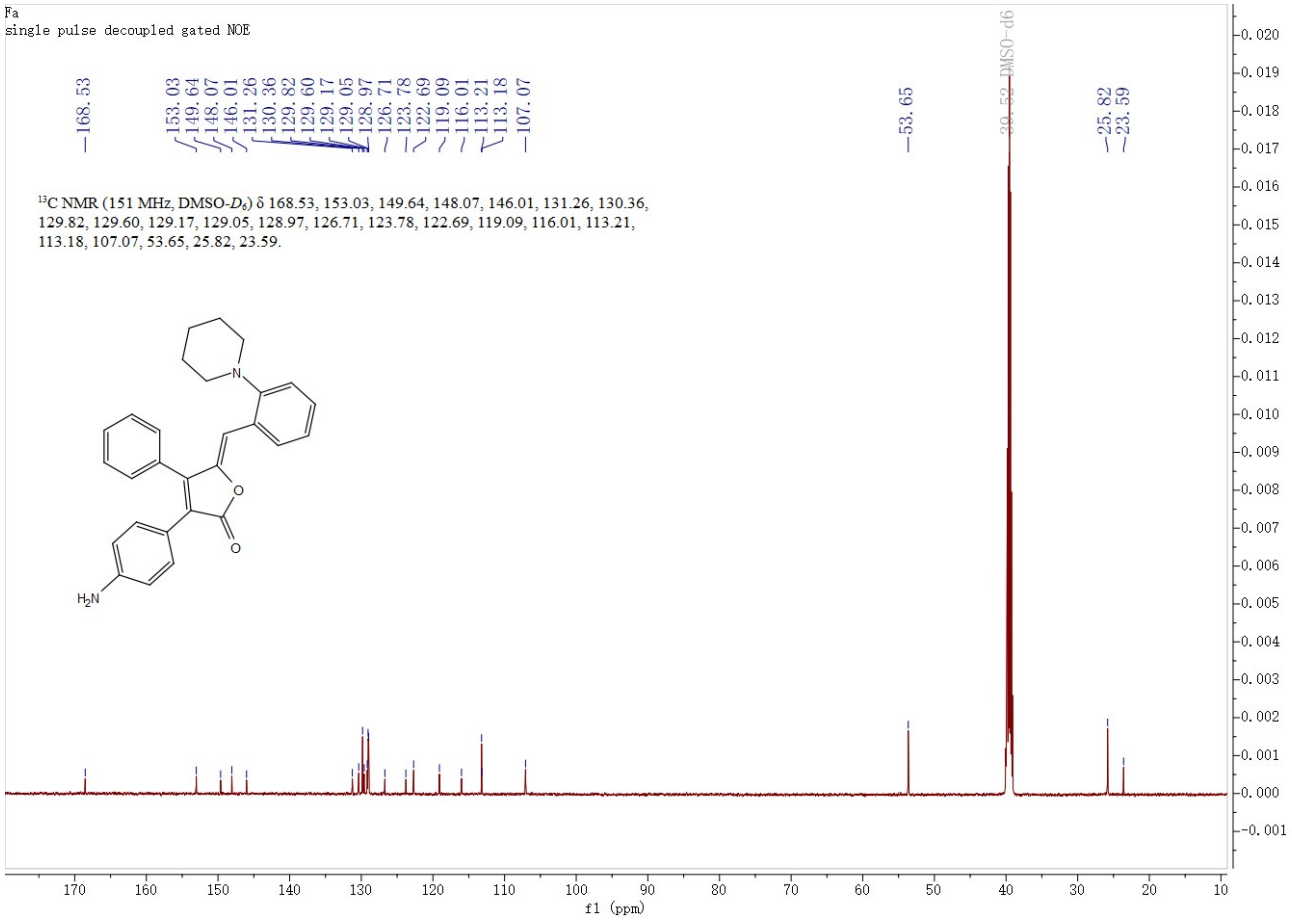

Figure S11. ^{13}C NMR of FA (151 MHz, DMSO-D_6).

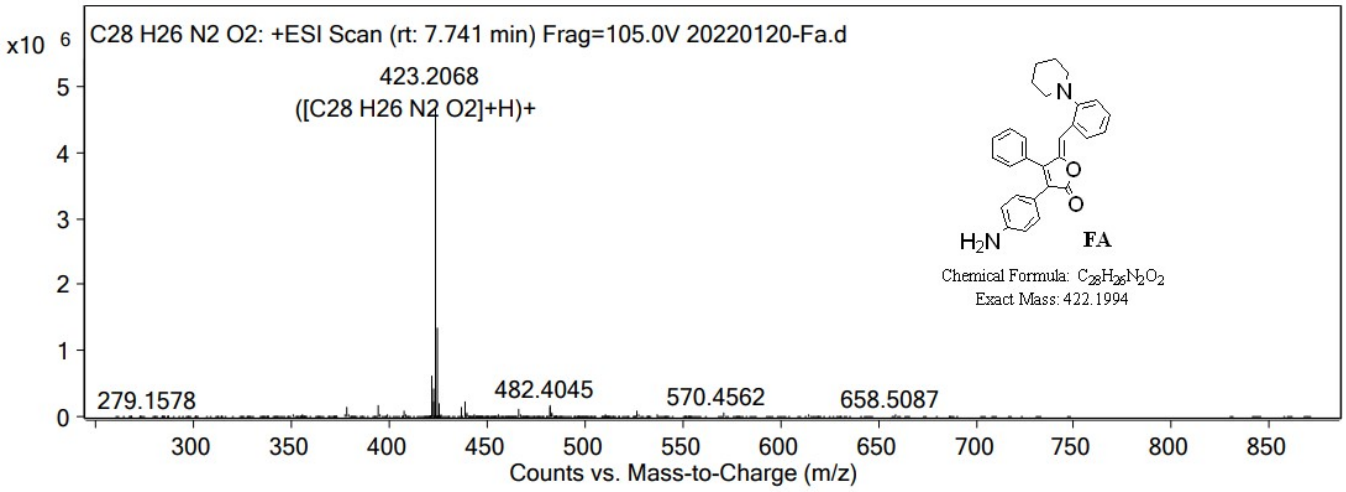

Figure S12. The HRMS spectra of FA.

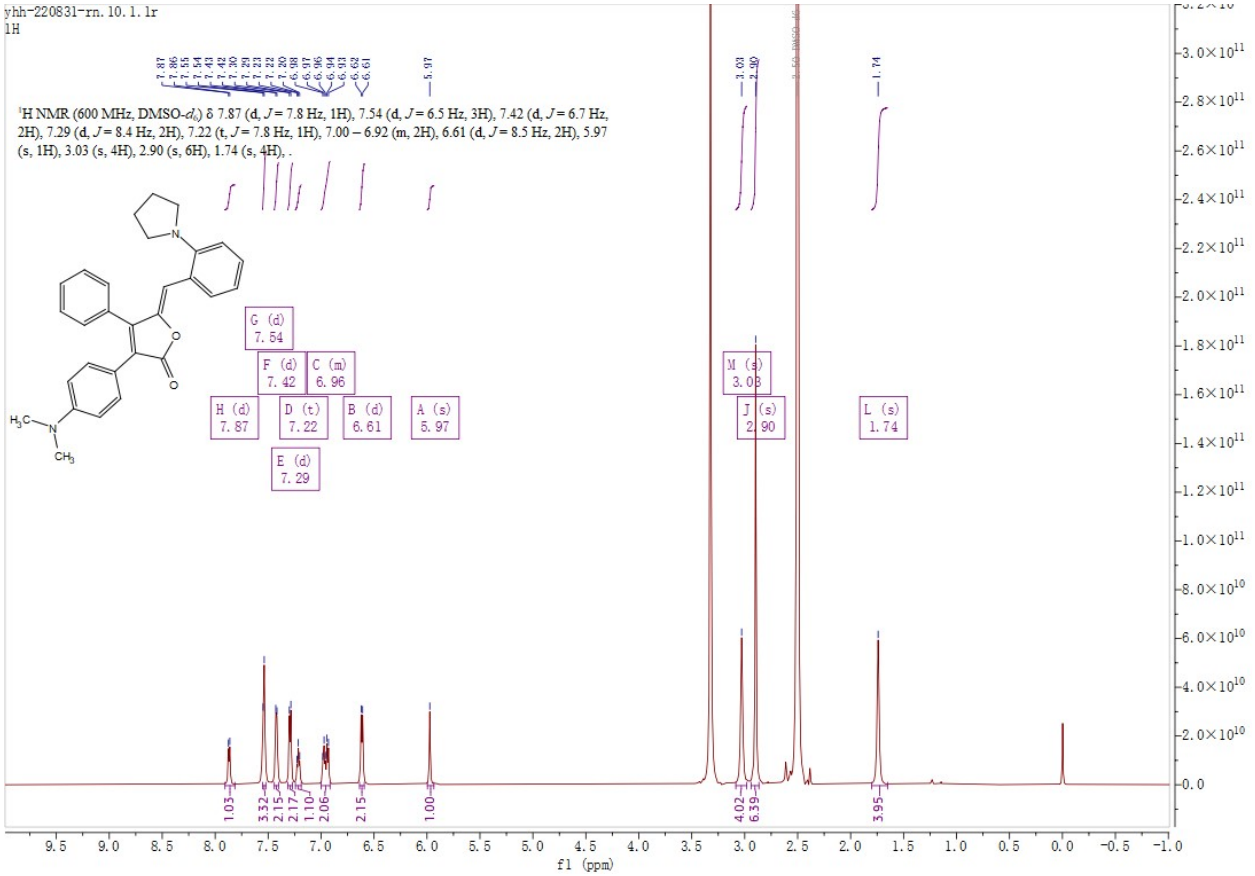

Figure S13. ^{1}H NMR of FB (600 MHz, DMSO-D_6).

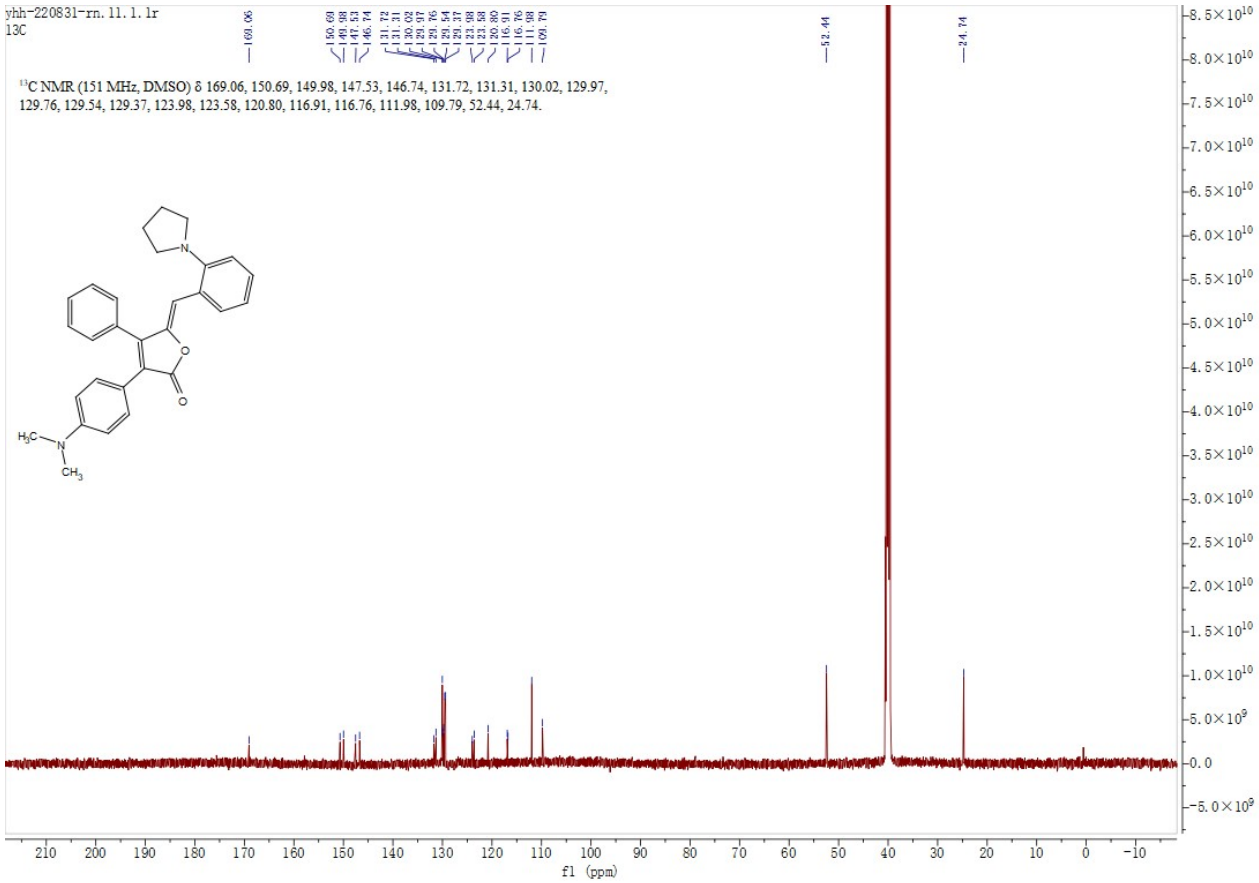

Figure S14. ^{13}C NMR of FB (151 MHz, DMSO-D_6).

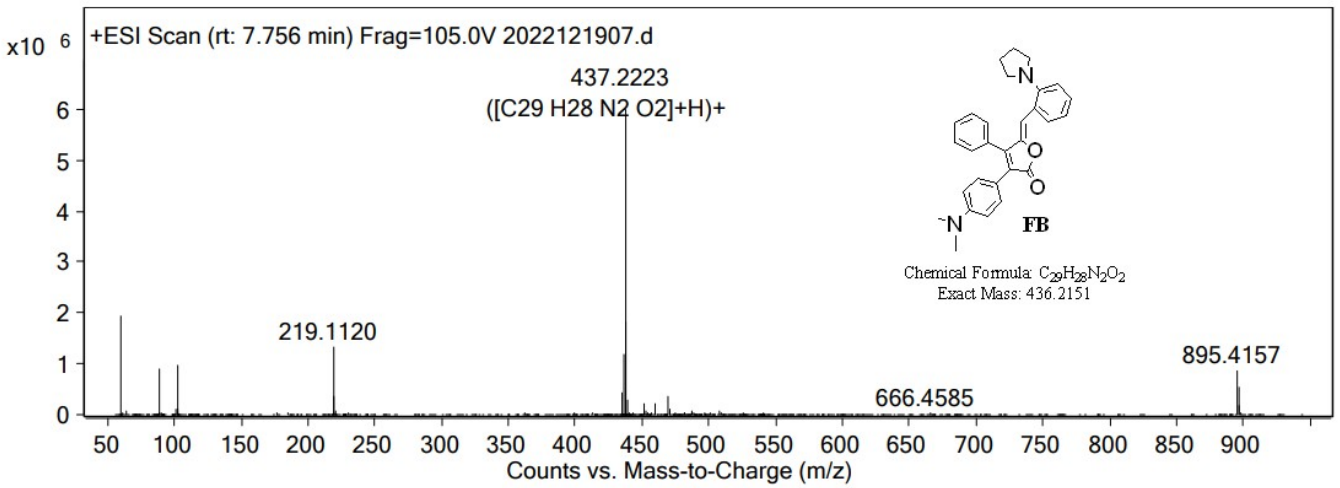

Figure S15. The HRMS spectra of FB.

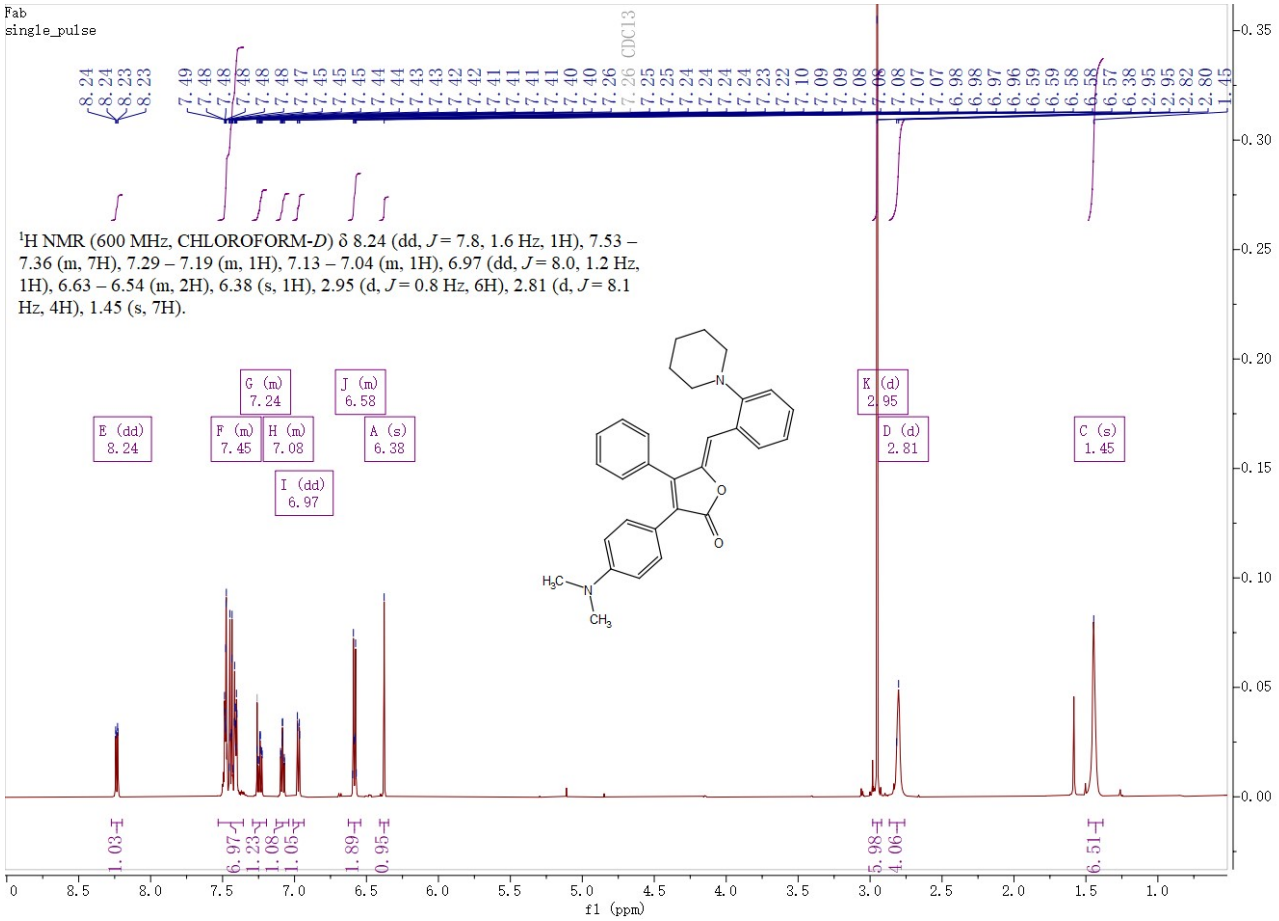

Figure S16. ^{1}H NMR of FAB (600 MHz, chloroform-*D*).

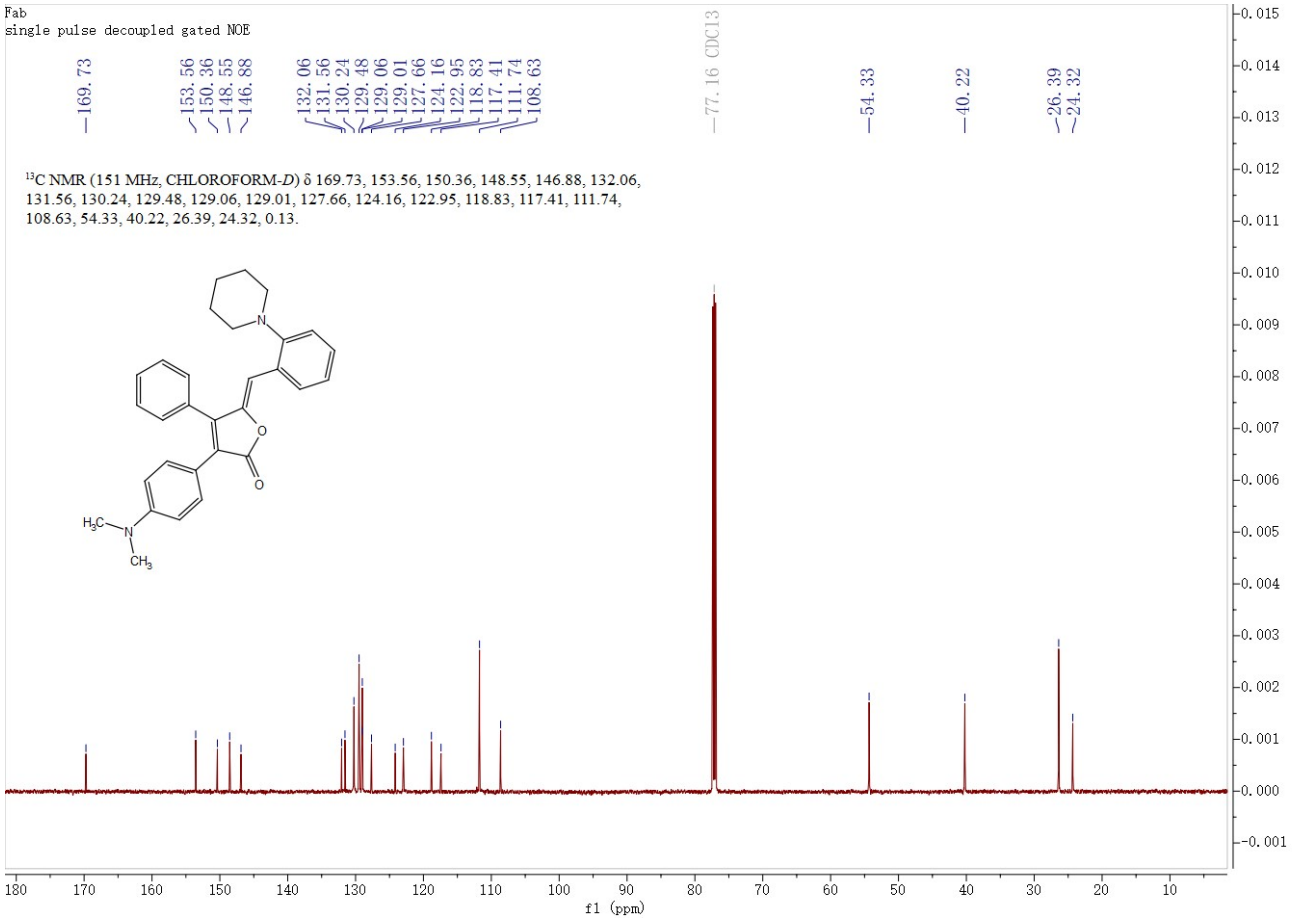

Figure S17. ^{13}C NMR of FAB (151 MHz, chloroform-*D*).

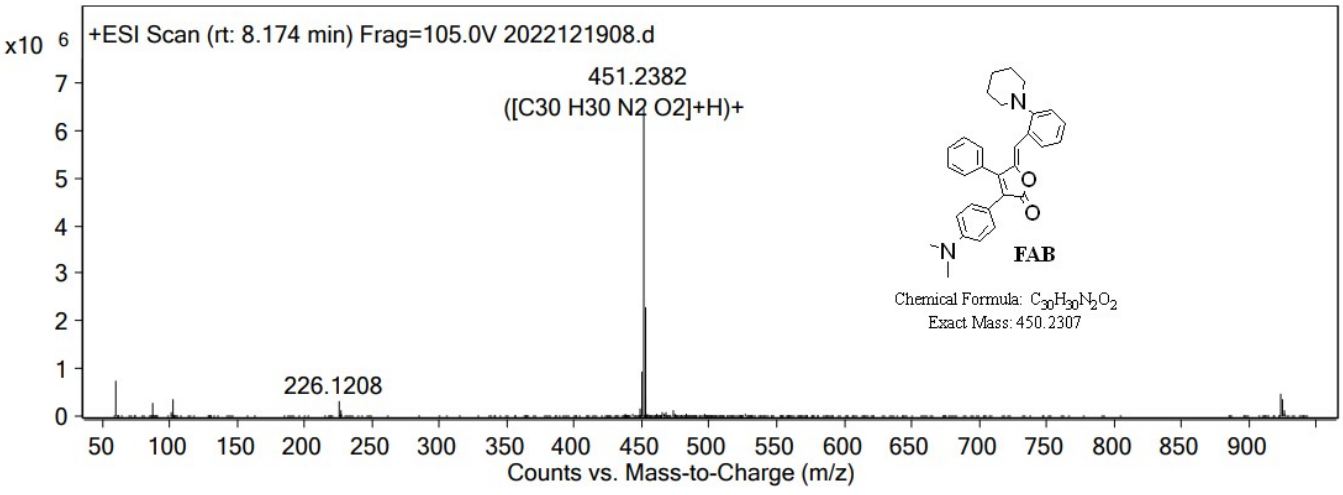

Figure S18. The HRMS spectra of FAB.

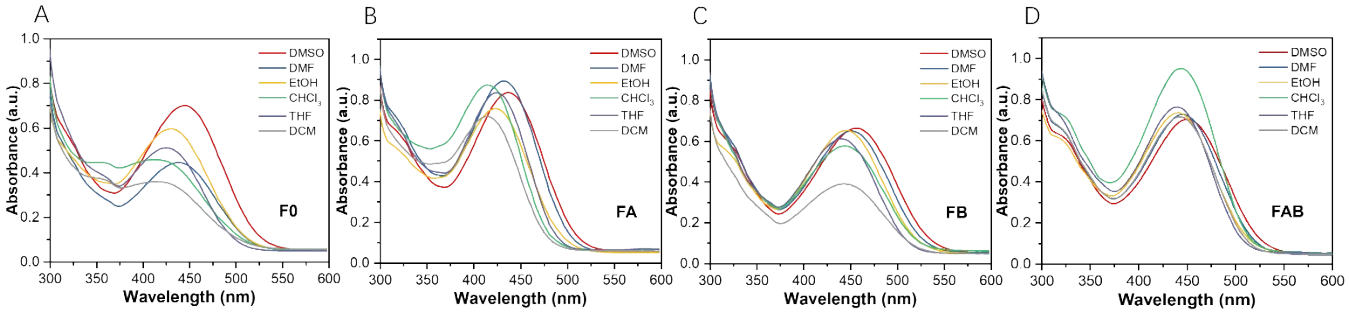

Figure S19. Absorption spectra of compounds F0(A), FA(B), FB(C) and FAB(D) in different solvents. (c = 50 μM) .

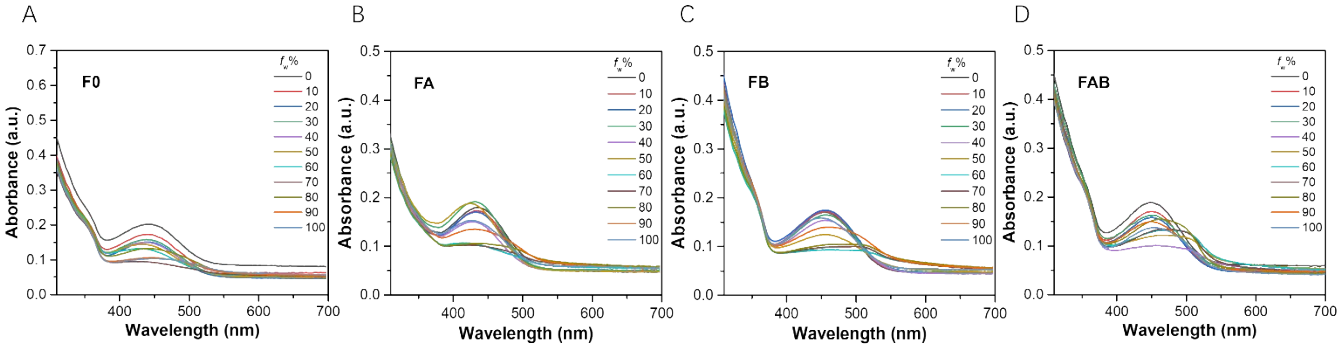

Figure S20. Absorption spectra of compounds F0(A), FA(B), FB(C) and FAB(D) in water−DMSO mixtures with different water fractions (c = 10 μM).

Table S1. Crystal data and structure refinement for FA, FB and FAB.

Identification code	FA	FB	FAB
Empirical formula	$C_{28}H_{26}N_2O_2$	$C_{29}H_{28}N_2O_2$	$C_{30}H_{30}N_2O_2$
Formula weight	422.51	436.53	450.56
Temperature/K	209.97(10)	301(2)	293(2)
Crystal system	monoclinic	triclinic	monoclinic
Space group	$P2_1/c$	P-1	$P2_1/c$
a/Å	19.0477(8)	6.4373(8)	6.5167(2)
b/Å	9.9685(4)	10.0005(11)	21.0675(9)
c/Å	11.9731(5)	21.835(2)	17.9822(7)
α/°	90	93.642(9)	90
β/°	90.239(4)	94.017(9)	95.495(4)
γ/°	90	106.807(10)	90
Volume/Å^3	2273.40(16)	1337.1(3)	2457.44(16)
Z	4	2	4
ρ_{calc}g/cm^3	1.234	1.084	1.218
μ/mm^{-1}	0.078	0.068	0.38
F(000)	896	464	960
Crystal size/mm^3	0.43×0.35×0.21	0.32×0.25×0.22	0.16×0.1×0.08
Radiation	MoKα (λ = 0.71073)	MoKα (λ = 0.71073)	MoKα (λ = 1.3405)
2Θ range for data collection/°	4.276 to 58.614	3.754 to 59.288	5.632 to 120.988
Index ranges	-24 ≤ h ≤ 24, -12 ≤ k ≤ 13, -16 ≤ l ≤ 16	-8 ≤ h ≤ 7, -12 ≤ k ≤ 13, -29 ≤ l ≤ 25	-8 ≤ h ≤ 6, -26 ≤ k ≤ 26, -23 ≤ l ≤ 21
Reflections collected	14206	11639	18646
Independent reflections	4981 [R_{int} = 0.0362, R_{sigma} = 0.0385]	5784 [R_{int} = 0.0428, R_{sigma} = 0.0718]	5481 [R_{int} = 0.0512, R_{sigma} = 0.0568]
Data/restraints/parameters	4981/0/292	5784/303/300	5481/189/340
Goodness-of-fit on F^2	1.051	0.992	1.026
Final R indexes [I>=2σ (I)]	R_1 = 0.0506, wR_2 = 0.1169	R_1 = 0.0803, wR_2 = 0.2347	R_1 = 0.0630, wR_2 = 0.1652
Final R indexes [all data]	R_1 = 0.0788, wR_2 = 0.1297	R_1 = 0.1334, wR_2 = 0.2722	R_1 = 0.1037, wR_2 = 0.1863
Largest diff. peak/hole / e Å^{-3}	0.36/-0.28	0.32/-0.20	0.17/-0.16

Table S2. Fractional Atomic Coordinates (×10^4) and Equivalent Isotropic Displacement Parameters (Å^2×10^3) for FA. U_{eq} is defined as 1/3 of the trace of the orthogonalised U_{IJ} tensor.

Atom	*x*	*y*	*z*	U(eq)
O2	7430.7(6)	8027.7(11)	4772.5(9)	30.1(3)
O1	6835.6(6)	8901.0(11)	6207.3(10)	35.4(3)
N2	8810.8(7)	5701.1(14)	1722.2(12)	35.5(3)
C8	6971.3(8)	7921.6(16)	5656.2(13)	27.6(3)
C10	7024.0(8)	5846.5(15)	4855.0(13)	26.9(3)
C7	6713.3(8)	6526.1(15)	5707.8(13)	27.2(3)
C4	6178.5(8)	6119.5(16)	6521.4(13)	28.6(3)
C9	7471.6(8)	6779.7(15)	4248.2(13)	27.9(3)
C17	7856.3(8)	6594.4(16)	3327.7(13)	29.0(3)
C11	6940.2(8)	4415.3(16)	4548.2(13)	29.5(4)
C18	8239.9(8)	7573.3(16)	2660.4(13)	29.7(4)
C3	6145.9(9)	6714.6(16)	7578.8(14)	32.6(4)
N1	4603.8(9)	5098(2)	8826.1(15)	62.5(6)
C2	5633.3(9)	6377.5(18)	8337.0(14)	35.6(4)
C19	8141.0(9)	8968.3(17)	2767.5(14)	35.1(4)
C23	8683.5(8)	7101.6(17)	1798.1(14)	31.8(4)
C16	7080.0(9)	3420.4(17)	5332.0(16)	40.0(4)
C1	5121.9(9)	5426.3(19)	8065.6(15)	39.7(4)
C5	5668.1(9)	5159.1(18)	6264.4(15)	38.2(4)
C12	6698.3(10)	4042.2(18)	3497.0(15)	43.1(4)
C20	8446.3(9)	9859.9(18)	2031.3(16)	40.9(4)
C22	8966.2(9)	8022.5(19)	1043.5(15)	41.2(4)
C21	8846.4(10)	9384(2)	1154.7(16)	45.0(5)
C28	9253.9(10)	5177.1(19)	2626.2(17)	43.5(5)
C6	5152.2(9)	4821(2)	7019.4(16)	44.9(5)
C24	9042.9(11)	5212(2)	632.7(17)	49.7(5)
C15	6979.7(11)	2079.6(19)	5071(2)	51.2(5)
C14	6729.2(12)	1722(2)	4029(2)	57.4(6)
C13	6585.4(12)	2703(2)	3245.6(18)	58.2(6)
C27	9233.3(12)	3649(2)	2653(2)	58.5(6)
C26	9465.2(12)	3091(2)	1533(2)	64.4(7)
C25	9026.3(12)	3686(2)	607(2)	63.5(6)

Table S3. Fractional Atomic Coordinates (×10^4) and Equivalent Isotropic Displacement Parameters (Å^2×10^3) for FB. U_{eq} is defined as 1/3 of the trace of the orthogonalised U_{IJ} tensor.

Atom	x	y	z	U(eq)
O001	6952(3)	3464.7(18)	2200.4(10)	59.9(5)
O002	4349(4)	2117(2)	2704.5(12)	77.7(7)
N003	11999(4)	6898(3)	936.6(13)	76.6(8)
C004	7001(4)	7155(3)	2514.8(13)	50.4(6)
C005	6577(4)	5617(3)	2501.0(13)	49.5(6)
C006	3375(4)	4820(3)	3166.5(13)	50.3(6)
C007	5016(4)	4659(3)	2762.5(13)	51.1(7)
C008	3563(4)	6071(3)	3511.0(14)	56.1(7)
C009	7793(4)	4887(3)	2144.7(13)	52.5(7)
N00A	-1458(5)	5286(3)	4298.4(16)	87.2(9)
C00B	5354(4)	7711(3)	2333.7(15)	59.6(7)
C00C	5271(5)	3273(3)	2579.0(15)	58.3(7)
C00D	10687(4)	4741(3)	1433.2(14)	61.1(8)
C00E	-56(5)	3867(3)	3602.2(15)	64.4(8)
C00F	126(5)	5134(3)	3936.9(14)	61.4(7)
C00G	1999(5)	6226(3)	3884.4(14)	61.4(8)
C00H	9385(4)	5405(3)	1794.7(14)	57.1(7)
C00I	1518(4)	3722(3)	3228.9(14)	59.6(7)
C00J	12106(5)	5556(4)	1035.9(14)	66.9(8)
C00K	9054(5)	8056(3)	2713.9(16)	64.5(8)
C00L	5739(6)	9139(3)	2338.2(17)	72.5(9)
C00M	7762(6)	10024(3)	2531.0(18)	79.2(10)
C00N	9429(5)	9491(3)	2709.2(19)	79.5(10)
C00O	10739(6)	3376(4)	1503.7(17)	78.6(10)
C00P	13648(6)	5005(5)	792.7(17)	86.0(11)
C00Q	-1383(6)	6630(4)	4588(2)	90.4(11)
C00R	13717(7)	3678(6)	892.2(19)	95.7(13)
C00S	-3259(6)	4113(4)	4411(2)	91.5(12)
C00T	12243(7)	2849(5)	1235.5(19)	94.2(12)
C00U	9988(7)	7042(5)	629(2)	104.0(13)
C00V	13750(8)	7897(5)	672(2)	114.4(15)
C00X	10492(10)	8552(6)	541(3)	141.6(18)
C00Y	12917(10)	9132(6)	606(3)	142.2(18)

Table S4. Fractional Atomic Coordinates (×10^4) and Equivalent Isotropic Displacement Parameters (Å^2×10^3) for FAB. U_{eq} is defined as 1/3 of the trace of the orthogonalised U_{IJ} tensor.

Atom	x	y	z	U(eq)
O001	2641(2)	8008.9(8)	7515.6(8)	61.2(4)
O002	4671(3)	8859.5(9)	7709.5(10)	77.1(5)
N003	-956(3)	5886.4(10)	6966.1(12)	65.2(6)
C004	5000(3)	8156.5(11)	6645.4(11)	51.5(5)
C005	3825(3)	7645.2(11)	6434.9(11)	50.9(5)
C006	6691(3)	8460.3(10)	6301.9(12)	52.1(5)
C007	2361(3)	7539.7(11)	6974.3(12)	53.7(5)
C009	4211(4)	8401.7(12)	7331.4(12)	58.2(6)
C00A	-1611(3)	6360.0(13)	7451.2(13)	62.1(6)
C00B	6909(4)	8404.2(11)	5538.2(12)	57.6(6)
C00C	988(3)	7070.4(12)	6992.5(12)	56.3(5)
C00D	10050(4)	9020.6(12)	5645.1(14)	61.6(6)
C00E	-566(3)	6946.5(12)	7499.2(13)	58.6(6)
C00F	8191(4)	8813.0(12)	6719.2(13)	60.4(6)
N00G	11708(4)	9275.5(14)	5334.5(14)	95.2(8)
C00H	9820(4)	9083.4(12)	6404.8(14)	65.0(6)
C00I	8519(4)	8675.5(12)	5222.5(13)	63.8(6)
C00K	-1199(4)	7408.0(15)	7987.0(14)	72.4(7)
C00L	-3298(4)	6274.6(17)	7863.3(17)	81.3(8)
C00M	979(4)	5574.0(14)	7229.4(17)	76.1(7)
C00O	-2506(4)	5420.6(15)	6669.3(19)	86.4(9)
C00P	-3915(5)	6742(2)	8316.9(18)	92.2(10)
C00Q	-2862(5)	7307.6(18)	8393.4(16)	86.9(9)
C00R	4700(20)	6463(4)	4558(5)	67(2)
C00W	2780(20)	6741(6)	4602(4)	70(2)
C00N	2439(15)	7121(6)	5210(6)	63.0(19)
C008	4017(17)	7223(6)	5774(6)	52(2)
C00J	5936(17)	6946(6)	5730(6)	64(2)
C00S	6280(20)	6566(4)	5121(6)	70(2)
C00T	13098(5)	9709.3(17)	5753(2)	93.9(10)
C00U	1812(5)	5193.9(17)	6615(2)	96.6(10)
C00V	11964(5)	9189(2)	4556.3(19)	101.0(10)
C00X	225(6)	4720.1(17)	6278(2)	107.1(11)
C00Y	-1766(6)	5058.9(17)	6039(2)	104.5(11)
C5	3800(30)	6542(4)	4465(4)	70(3)
C4	2110(20)	6909(6)	4608(5)	81(2)
C3	2157(15)	7259(7)	5265(7)	73(2)
C0	3891(17)	7240(7)	5779(6)	54(2)
C2	5580(17)	6873(6)	5636(6)	60.7(19)
C1	5540(20)	6524(4)	4979(6)	70(2)

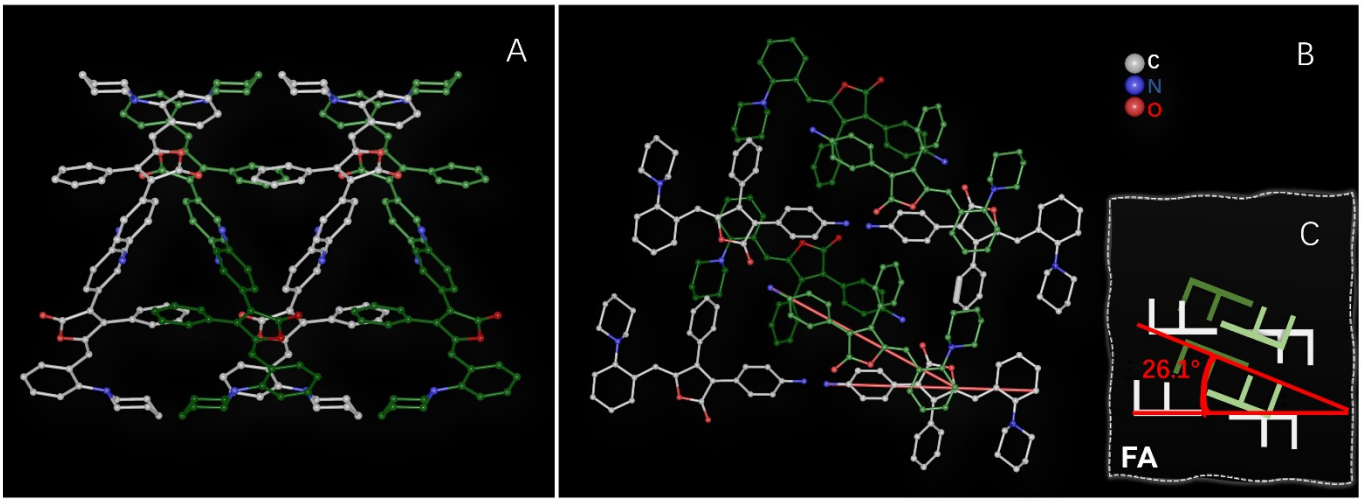

Figure S21. Stacking structure (A, B) and diagram(C) of FA.

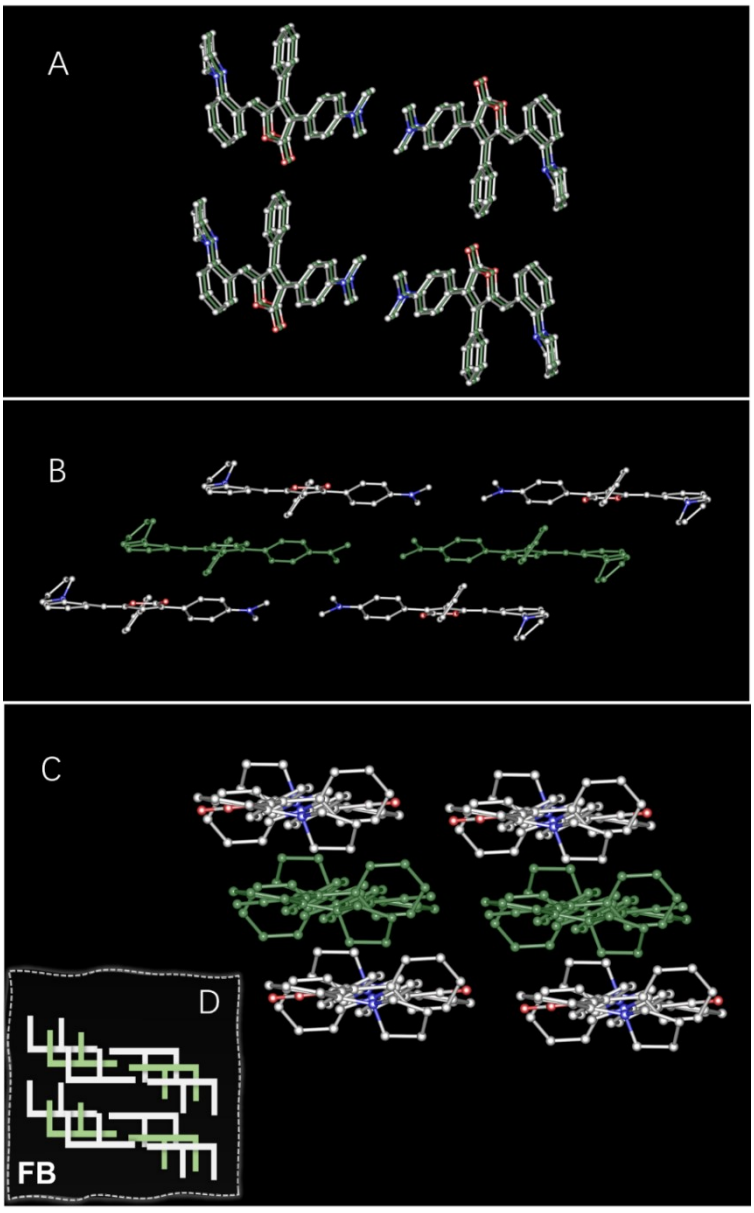

Figure S22. Stacking structure (A, B, C) and diagram(D) of FB.

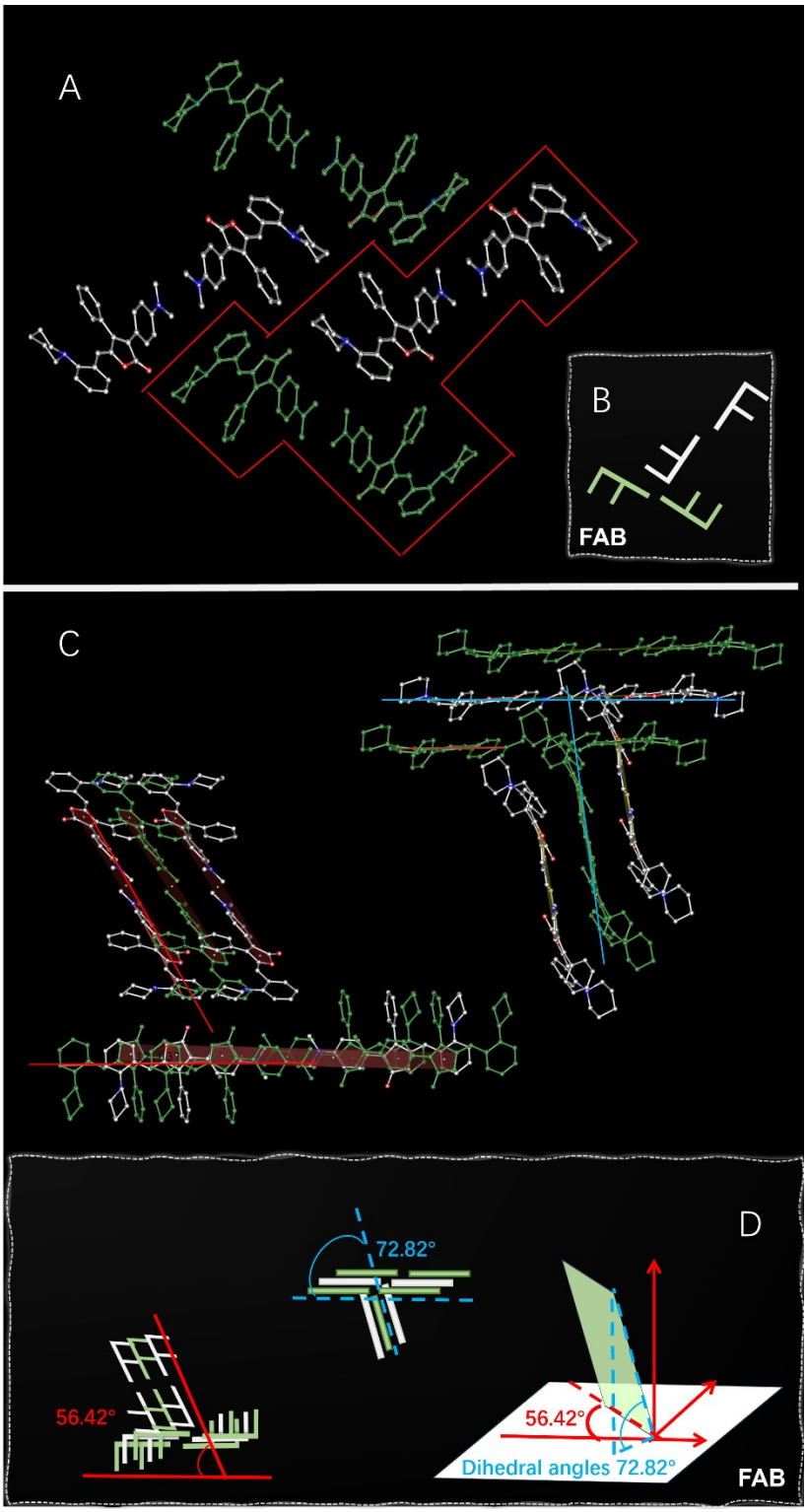

Figure S23. Stacking structure (A, C) and diagram (B, D) of FAB.

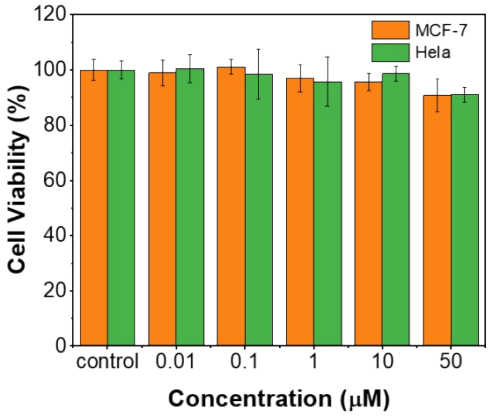

Figure S24. Cell viability values (%) estimated by CCK8 assays using MCF-7 and Hela cells, cultured in the presence of 0.01-50 μM of FAB for 24 h at 37 °C